Respiratory Research

RESEARCH

Open Access

Ubiquitination of angiotensin-converting enzyme 2 contributes to the development of pulmonary arterial hypertension mediated by neural precursor cell–expressed developmentally down-regulated gene 4-Like

Rui Wang[1,2†], Rui Wang[3†], Siqi Zhou[4†], Tianya Liu[2], Jingjing Dang[1,2], Qianmin Chen[2], Jingyu Chen[1] and Zhiping Wang[1,2*]

Abstract

Objectives In this study, we investigated whether neural precursor cell–expressed developmentally down-regulated gene 4-like (NEDD4L) is the E3 enzyme of angiotensin-converting enzyme 2 (ACE2) and whether NEDD4L degrades ACE2 via ubiquitination, leading to the progression of pulmonary arterial hypertension (PAH).

Methods Bioinformatic analyses were used to explore the E3 ligase that ubiquitinates ACE2. Cultured pulmonary arterial smooth muscle cells (PASMCs) and specimens from patients with PAH were used to investigate the crosstalk between NEDD4L and ACE2 and its ubiquitination in the context of PAH.

Results The inhibition of ubiquitination attenuated hypoxia-induced proliferation of PASMCs. The levels of NEDD4L were increased, and those of ACE2 were decreased in lung tissues from patients with PAH and in PASMCs. NEDD4L, the E3 ligase of ACE2, inhibited the expression of ACE2 in PASMCs, possibly through ubiquitination-mediated degradation. PAH was associated with upregulation of NEDD4L expression and downregulation of ACE2 expression.

Conclusions NEDD4L, the E3 ubiquitination enzyme of ACE2, promotes the proliferation of PASMCs, ultimately leading to PAH.

Keywords Pulmonary arterial hypertension, Neural precursor cell–expressed developmentally down-regulated gene 4-like, Ubiquitination, Angiotensin-converting enzyme 2, Pulmonary arterial smooth muscle cells

†Rui Wang 1, Rui Wang 2 and Siqi Zhou contributed equally to this work.

*Correspondence:
Zhiping Wang
zhpsqxt@126.com
[1]Graduate School, Nanjing Medical University, 101 Longmian Avenue, Jiangning District, Nanjing, Jiangsu, China
[2]Present address: Department of Anesthesiology, Affiliated Hospital of Xuzhou Medical University, No.99 Huaihai West Road, Xuzhou, Jiangsu, China
[3]Department of Orthopedics, Xuzhou Central Hospital, 199 Jiefang South Road, Quanshan District, Xuzhou, Jiangsu, China
[4]Department of Gastroenterology, Nanjing Drum Tower Hospital Clinical College of Jiangsu University, 321 Zhongshan Road, Drum Tower District, Nanjing, Jiangsu, China

Introduction

Pulmonary arterial hypertension (PAH) is a fatal disease characterized by a progressive increase in pulmonary vascular pressure [1]. The pulmonary vasculature suffers occlusive lesions, abnormal vasoconstriction, and pulmonary vascular resistance (PVR). Obstructive PVR in PAH increases right ventricular afterload, leading to right ventricular dysfunction and ultimately death [2]. The vascular cells of pulmonary arteries include inner endothelial cells, media smooth muscle cells, and adventitial fibroblasts. A proliferative and apoptosis-resistant phenotype of pulmonary artery smooth muscle cells (PASMCs) results in medial thickening and occlusive vascular lesions [3, 4]. Hypoxia, a fundamental stimulus in the pulmonary microenvironment, triggers a cascade of cellular and molecular events that culminate in PASMCs hyperplasia [5]. This proliferative response is orchestrated by a complex interplay of growth factors, cytokines, and signaling pathways, ultimately leading to an imbalance in the homeostatic mechanisms governing vascular architecture [6]. This proliferation serves as the cornerstone of PVR, a pathological hallmark in the progression of PAH [7]. However, there are currently no effective treatments to stop its development [8]. According to our previous study, decreased expression of angiotensin-converting enzyme 2 (ACE2) promotes expression of focal adhesion kinase, which in turn leads to increased proliferation of PASMCs, resulting in PVR and ultimately PAH [9].

Identified in 2000 [10], ACE2—which shares approximately 61% sequence homology with the catalytic domains of its homolog ACE1—primarily hydrolyses Ang II into Ang-(1–9) and Ang-(1–7) with high efficiency [11]. Both Ang-(1–9) and Ang-(1–7) promote vasodilation and decrease cell growth and inflammatory responses [12, 13]. Since upregulation of Ang II expression and signaling has been reported in PASMCs of remodeled vessels in the lungs of patients with idiopathic PAH, infusion of recombinant human ACE2 (NCT01884051) has been shown to offer potential hemodynamic benefits for PAH treatment [11, 14]. However, the mechanisms by which ACE2 expression decreases are still unclear [15].

Ubiquitination is key to the dynamic regulation of programmed cell death. Dysregulation of this process by regulating enzymes and targets of fundamental cellular processes involved in cell death and inflammation can lead to disease consequences [16, 17]. The ubiquitin-proteasome system regulates protein degradation and the development of PAH, but knowledge about how E3 ubiquitin ligase affects ACE2 expression is limited [18]. Ubiquitinated degradation of ACE2 is one of the mechanisms of pneumonia in studies of SARS-CoV-2 infection [19, 20]. Similar conclusions have been reached in studies of hypertension [21, 22]. An increase in pulmonary intravascular pressure is associated with lung inflammation in PAH patients [23, 24]. Thus, we hypothesized that the decrease in ACE2 is associated with its degradation via ubiquitination in PAH.

Neural precursor cell–expressed developmentally down-regulated gene 4-like (NEDD4L, also known as NEDD4-2) is the dominant E3 ligase of the NEDD4 family, and related signaling plays fundamental roles in cardiovascular diseases [25]. MG-132, a protease inhibitor, can inhibit proteases in the ubiquitination system, allowing proteins that should be degraded by ubiquitination to survive [26]. In a PAH model, the expression of NEDD4L was increased, while these changes were suppressed by treatment of PAH rats with MG-132 [27]. However, it is unclear whether NEDD4L, a possible E3 ligase of ACE2, exacerbates PAH by degrading ACE2.

Materials and methods

Isolation and culture of PASMCs

This study was approved by the Animal Ethics Committee of Xuzhou Medical University (approval number: 2022105068). C57BL/6 wild-type male mice aged 6–8 weeks were obtained from Beijing Weitong Lihua Experimental Animal Technology Co., Ltd. The animal license number is SCXK (Beijing) 2021-0011. Mice were anesthetized with pentobarbital sodium prior to euthanasia by right ventricular haemorrhage. PASMCs were obtained using an improved method of tissue piece inoculation via digestion with trypsin [28]. Cell morphology was observed under an inverted phase-contrast microscope, and a cell growth curve was generated by counting the cells. Immunofluorescence (IF) staining for α-smooth muscle actin (α-SMA) was used to assess the cell type and purity of PASMCs (shown in green, Supplementary Fig. 1). PASMCs were cultured in Dulbecco's modified Eagle's medium (DMEM) containing 15% fetal bovine serum, 100 U/mL penicillin, and 100 U/mL streptomycin, and placed in an incubator at 37 °C, saturated humidity, and 5% CO_2. PASMCs were subjected to hypoxic treatment in a hypoxic chamber (MIC-101, Billups-Roche, USA) with an O_2 concentration of 4% for 24 h.

The reagents used and their commercial sources were as follows: cycloheximide (CHX; 239763, Sigma–Aldrich, Germany); MG132 (M7449, Sigma–Aldrich, Germany); DMEM (iCell-0001, iCell Bioscience, China); anti–α-SMA (ab7817, Abcam, UK); anti-ACE2 (21115-1-AP, Proteintech, USA); anti–glyceraldehyde-3-phosphate dehydrogenase (GAPDH; 60004-1-Ig, Proteintech, USA); anti-NEDD4L (ab46521, Abcam, UK); anti–caspase-3 and anti-mouse double minute 2 (MDM2; ab259265, Abcam, UK); Cell Counting Kit-8 (CCK-8; HY-K0301, MedChemExpress, USA); coraLite488-conjugated goat anti-mouse immunoglobulin (Ig)G (H+L) (SA00013-1,

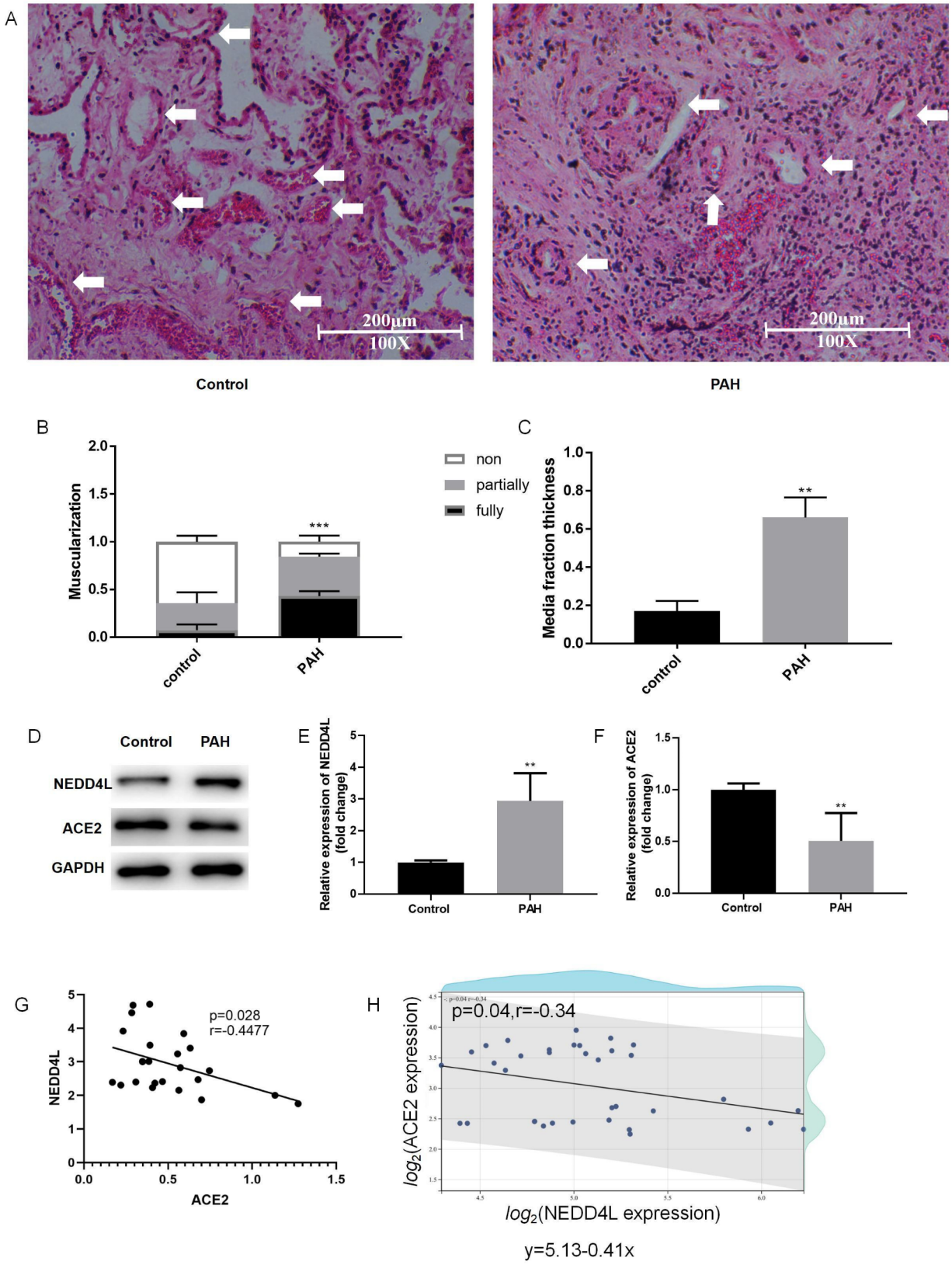

Fig. 1 (See legend on next page.)

(See figure on previous page.)

Fig. 1 The protein expression levels of NEDD4L and ACE2 negatively correlate under hypoxia. We collected lung tissue samples from patients diagnosed with PAH caused by hypoxia. These samples underwent HE staining for histological assessment and western blot analysis to quantify protein expression levels. HE-stained histological images of pulmonary arteries (**A**), with the white arrow indicating the pulmonary artery (diameter ≤ 200 μm). Muscularization (**B**) and the proportions of media fraction thickness (**C**) were determined by selecting 20–40 pulmonary arterioles with a diameter of ~ 50 μm. The protein expression levels of NEDD4L (**D**, **E**) and ACE2 (**D**, **F**) were detected by western blotting, and GAPDH was used as an internal reference. The correlation between the expression in the samples (**G**) and that in the GEO database (**H**) was analyzed (GSE22356; https://www.ncbi.nlm.nih.gov/geo/query/acc.cgi?acc=GSE22356). GEO RNA-Sequencing dataset (GSE22356) was generated from peripheral blood mononuclear cells from patients with and without scleroderma-associated pulmonary hypertension. $N = 4$, $^{**}P < 0.01$, $^{***}P < 0.001$. NEDD4L, neural precursor cell–expressed developmentally downregulated gene 4-like; ACE2, angiotensin-converting enzyme 2; PAH, pulmonary arterial hypertension; GAPDH, glyceraldehyde-3-phosphate dehydrogenase; GEO, Gene Expression Omnibus

Proteintech, USA); and an EdU staining kit (KGA331, Keygen Biotech, China).

Human lung samples

This study was also approved by the Ethics Committee of the Affiliated Hospital of Xuzhou Medical University (approval number: XYFY2022-KL401-01) and registered in the clinical trial center (registration number: ChiCTR2200066496). These samples were obtained from the Affiliated Hospital of Xuzhou Medical University and Wuxi People's Hospital. The patients/participants provided written informed consent to participate in the study. The authors affirm that human participants provided informed consent for publication of the images in Fig. 1A. After the subjects provided informed consent and agreed to undergo lung biopsy, lung biopsy was performed to obtain lung tissue samples from six PAH patients who underwent lung transplantation and six patients who underwent pneumonectomy for benign nodules without PAH. Based on ethical considerations, we selected patients with PAH who underwent lung transplantation with a primary diagnosis of hypoxic PAH for the PAH group and patients who underwent pulmonary nodule resection with a primary diagnosis of benign pulmonary nodules for the control group.

Cell transfection

First, 20 nM NEDD4L-siRNA or scramble control RNA, designed and synthesized by GUANGZHOU IGE Biotechnology Ltd. (China), was transfected into PASMCs at a concentration (Every 1.5 μL Lipofectamine RNAi Max Reagent with 25 μL OPTI-MEM) of Lipofectamine RNAi Max (13778150, Invitrogen, USA). NEDD4L-pEGFP-N1 and ACE2-pEGFP-N1 were designed by SnapGene (https://www.snapgene.com/) and constructed by Biohealth. NEDD4L-pEGFP-N1, ACE2-pEGFP-N1, and vector were transfected into PASMCs using Lipofectamine 3000 (L3000001, Invitrogen) diluted with OPTI-MEM (11058021, Gibco, USA).

In silico method

UbiBrowser (http://ubibrowser.ncpsb.org) was used to predict the E3 ligases. Based on the combination of confidence and evidence models, the species selected was *Homo sapiens*, and a list of putative ACE2 E3 ligases is shown in Fig. 2A. To develop the correlation scatter plot shown in Fig. 1H, we analyzed a gene expression omnibus (GEO) RNA-sequencing dataset (GSE22356) generated from peripheral blood mononuclear cells from patients with and without scleroderma-associated pulmonary hypertension using the online tool Sangerbox (http://sangerbox.com/home.html).

Western blot analysis and quantitative PCR

Cells or tissues were lysed in radioimmunoprecipitation assay (RIPA) lysis buffer (P0013B, Beyotime Biotechnology, China) supplemented with protease inhibitors (HY-B0496, MedChemExpress). Lysates were resolved by sodium dodecyl sulfate–polyacrylamide gel electrophoresis (SDS–PAGE; P0012A, Beyotime Biotechnology) on a 10% gel and immunoblotted with antibodies, as indicated. For immunoprecipitation, the lysates were incubated with the described antibodies at 4 °C for 12 h, followed by 2 h of incubation at 25 °C with diluted horseradish peroxidase (HRP)-conjugated goat anti-mouse IgG (1:1,000; 91196, Cell Signaling, USA) or goat anti-rabbit IgG (1:3,000; 7074, Cell Signaling, USA). The immunoprecipitation products were observed by gel imaging (AlphaImager HP, ProteinSimple, USA) after using enhanced chemiluminescence (ECL) developer (WBKLS, Millipore Corporation, USA).

Coimmunoprecipitation (Co-IP) assays were carried out using a Co-IP kit (Bes3011, BerSinBio, China) following the manufacturer's protocols. HEK293 cells were transfected with ACE2 and ubiquitin-overexpressing plasmids (1 μg/mL) for 48 h, and control-siRNA and NEDD4L-siRNA (20 nM) were added for 24 h. After that, PASMCs or HEK293 cells were treated with MG132 for 10 h. Then, PASMCs or HEK293 cells were harvested and lysed. Antibodies (5 g) or IgG (5 L) were incubated with cell lysates at 4 °C overnight and then incubated with protein A/G magnetic beads at room temperature for 3 h. Finally, the IP products were washed with NETN buffer before being resolved by SDS–PAGE and immunoblotting (IB) with the indicated antibodies.

For qPCR, RNA was extracted from homogenized tissue or cells by using TRIzol reagent (T9424, Sigma–Aldrich, Germany). qPCR was performed using ChamQ

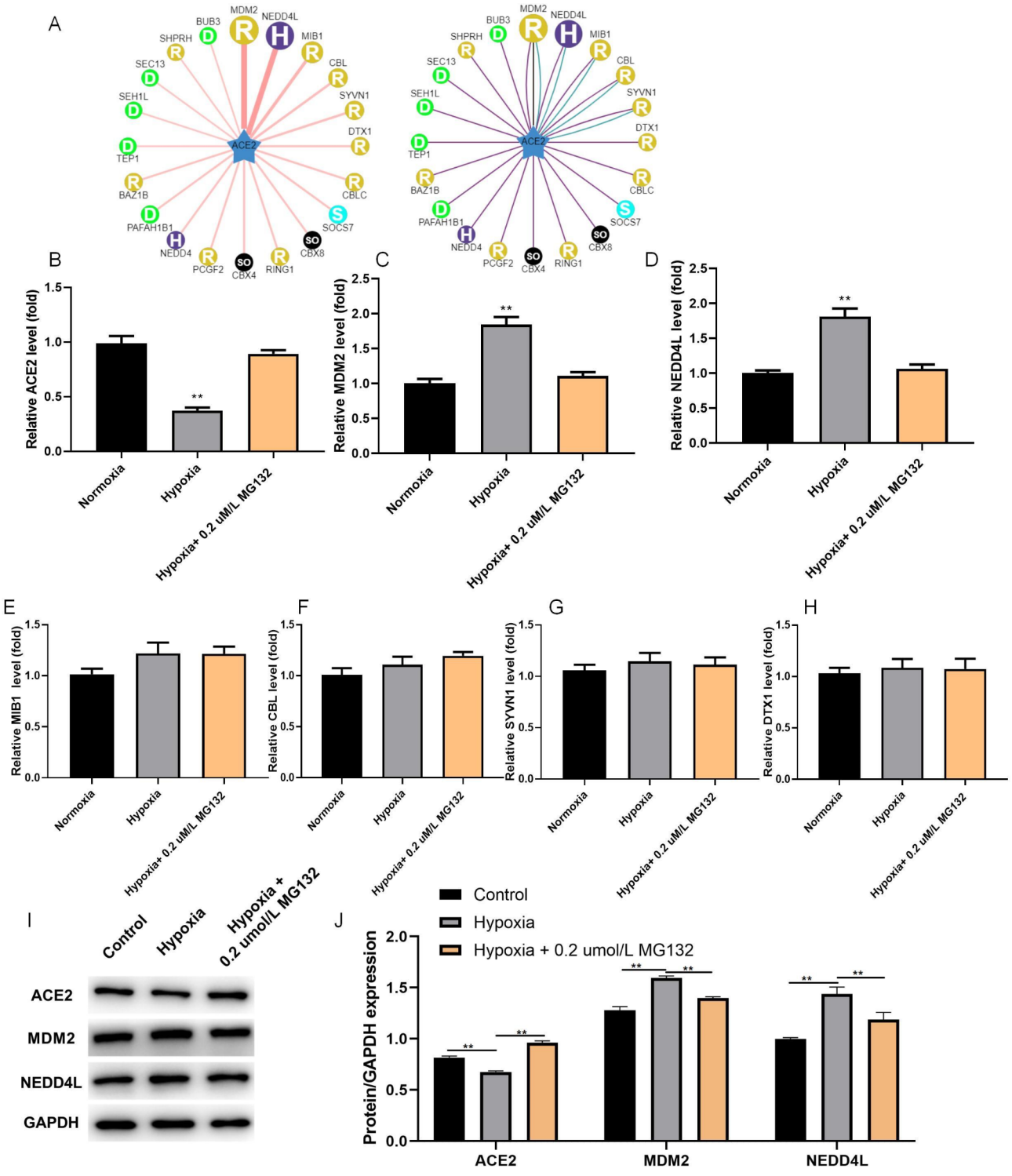

Fig. 2 NEDD4L may be the E3 ubiquitin ligase of ACE2 and inhibit the expression of ACE2 in PAH. In the network view, a node is positioned in the center of the canvas, showing the putative substrate ACE2, which is surrounded by nodes revealing predicted E3 ligases. The node colors and characteristics denote the E3 ligase type, with the edge width and node size representing the confidence score. In the confidence mode (**A**), both edge width and node size positively correlate with the UbiBrowser score. The top 1 to 6 genes were selected for qPCR to observe the effect of hypoxia and MG-132 on mRNA expression (**B-H**), and then, NEDD4L and MDM2 were selected for western blot analysis to observe the effect of hypoxia and MG-132 on protein expression. GAPDH was used as an internal reference (**I-J**). $n = 6$, $^{**}P < 0.01$. NEDD4L, neural precursor cell–expressed developmentally downregulated gene 4-like; ACE2, angiotensin-converting enzyme 2; PAH, pulmonary arterial hypertension; qPCR, quantitative PCR; MDM2, mouse double minute 2; GAPDH, glyceraldehyde-3-phosphate dehydrogenase

SYBR color qPCR master mix (Q411, Nanjing Novozan Biotechnology, China) and HiScript® II 1st strand cDNA synthesis kit (R211, Nanjing Novozan Biotechnology, China) with thioredoxin-binding protein (TBP) as an internal control. The relative gene expression was quantified by the ΔΔCt method. The sequences of primers used for qPCR are listed in Supplemental Table S1.

Histology

The pulmonary tissue was fixed with 4% paraformaldehyde (P0099, Beyotime Biotechnology, China) at 25 °C for 24 h, dehydrated using an ascending ethanol gradient, embedded in paraffin, and cut into 4-μm-thick sections. The sections were dewaxed using xylene, rehydrated with a descending graded ethanol series, stained with hematoxylin–eosin (HE; C0105, 0.5% hematoxylin for 5 min followed by 0.5% eosin for 1 min, both at 25 °C), hydrated with a graded alcohol series, and dehydrated with xylene. Images were acquired using an inverted light microscope (magnification, ×400; model, Leica DMi8; Leica Microsystems GmbH, Germany) under white light. Pulmonary arterioles with a diameter of ~50 μm were examined using Image-Pro Plus (version 6.0; Media Cybernetics, USA). The pulmonary artery comprises three layers: the inner, middle (muscular), and outer layers. The total diameter and media thickness of pulmonary arterioles were measured separately using HE staining, and the proportions of media fraction thickness was calculated by dividing the latter by the former [29].

IF and EdU staining (C0081, Beyotime Biotechnology, China) of PASMCs were performed on frozen cell sections. The instructions for EdU staining were followed. For IF staining, the cells were fixed in 4% paraformaldehyde at 4 °C for 30 min. Triton X-100 (0.5%, 9036-19-5, Sigma–Aldrich, Germany) was mixed with phosphate-buffered saline (PBS; C0221A, Beyotime Biotechnology, China) at a ratio of 1:1, and 10% goat serum (C0265, Beyotime Biotechnology, China) was added to the mixture, which was blocked for 120 min. The cells were incubated with anti-ACE2 antibody and coraLite488-conjugated goat anti-rabbit IgG (H+L) (P0176-1, Beyotime Biotechnology, China), and stained with DAPI (DAPI: PBS=1:1000, C1005, Beyotime Biotechnology, China), after which one drop of Fluoromount-G (P0176-3, Beyotime Biotechnology, China) was added to complete IF staining. Images were acquired using an inverted light microscope (magnification, ×100; model, Leica DMi8; Leica Microsystems GmbH, Germany).

Flow cytometry

After collection, PASMCs were stained with fluorescein isothiocyanate (FITC)-conjugated annexin V and propidium iodide (PI) in accordance with the manufacturer's instructions (Annexin V-FITC apoptosis assay kit, abs50001, Absin, China). By comparing the fluorescence intensity distribution of PASMCs, the proportion of apoptotic cells was quantitatively analyzed. The percentage of apoptotic cells was defined as the sum of early apoptotic cells and late apoptotic cells.

Statistical analyses

All the statistical analyses were performed with SPSS 22.0 or GraphPad Prism 8.0.2 software. All experiments were performed at least thrice with similar results. Initially, the datasets were analyzed for normality using the Shapiro–Wilk test ($P<0.05$) and for equal variance using the F test ($P>0.05$). For normally distributed data, two-tailed Student's t tests were used to compare two groups, and one-way ANOVA with the Bonferroni post-hoc correction was used for multiple groups. Two-way ANOVA was used in Fig. 1B for comparisons between two independent groups. Pearson correlation analysis was used in Fig. 1G and H. For non-normally distributed data or experiments with small sample sizes ($n<5$), the Mann–Whitney U test was used to compare two groups, and the Kruskal–Wallis test was used for comparisons among multiple groups. The data are expressed as the mean±standard error of the mean (SEM), and $P<0.05$ was considered to indicate statistical significance.

Results

Inhibition of ubiquitination attenuates hypoxia-induced proliferation of PASMCs

Compared with normoxia, hypoxia promoted cell viability of PASMCs, and MG132 inhibited this effect in a dose-dependent manner (Fig. 3A). Flow cytometry revealed that hypoxia inhibited the apoptosis of PASMCs, while MG132 promoted PASMCs apoptosis (Fig. 3C and F). Moreover, hypoxia inhibited the expression of ACE2 and caspase-3 in PASMCs, while MG132 increased their expression in a dose-dependent manner (Fig. 3B and D, and 3E). We tentatively speculate that the inhibition of ubiquitination attenuates hypoxia-induced PASMCs proliferation, possibly by inhibiting cell proliferation and promoting apoptosis.

NEDD4L may bind to ACE2 and reduce its expression in PAH via ubiquitination

UbiBrowser (http://ubibrowser.ncpsb.org) was used to predict the E3 ubiquitin ligase of ACE2 (Fig. 2A). The mRNA and protein expression levels of were decrease in response to hypoxic treatment, whereas they showed an increase following treatment with MG132(Fig. 2B, I, J). The mRNA and protein expression levels of MDM2 and NEDD4L were increased in hypoxia-treated PASMCs, whereas the mRNA and protein expression levels were decreased after MG132 treatment (Fig. 2C-D and I-J). The mRNA expression of ligases 3 to 6 did not change

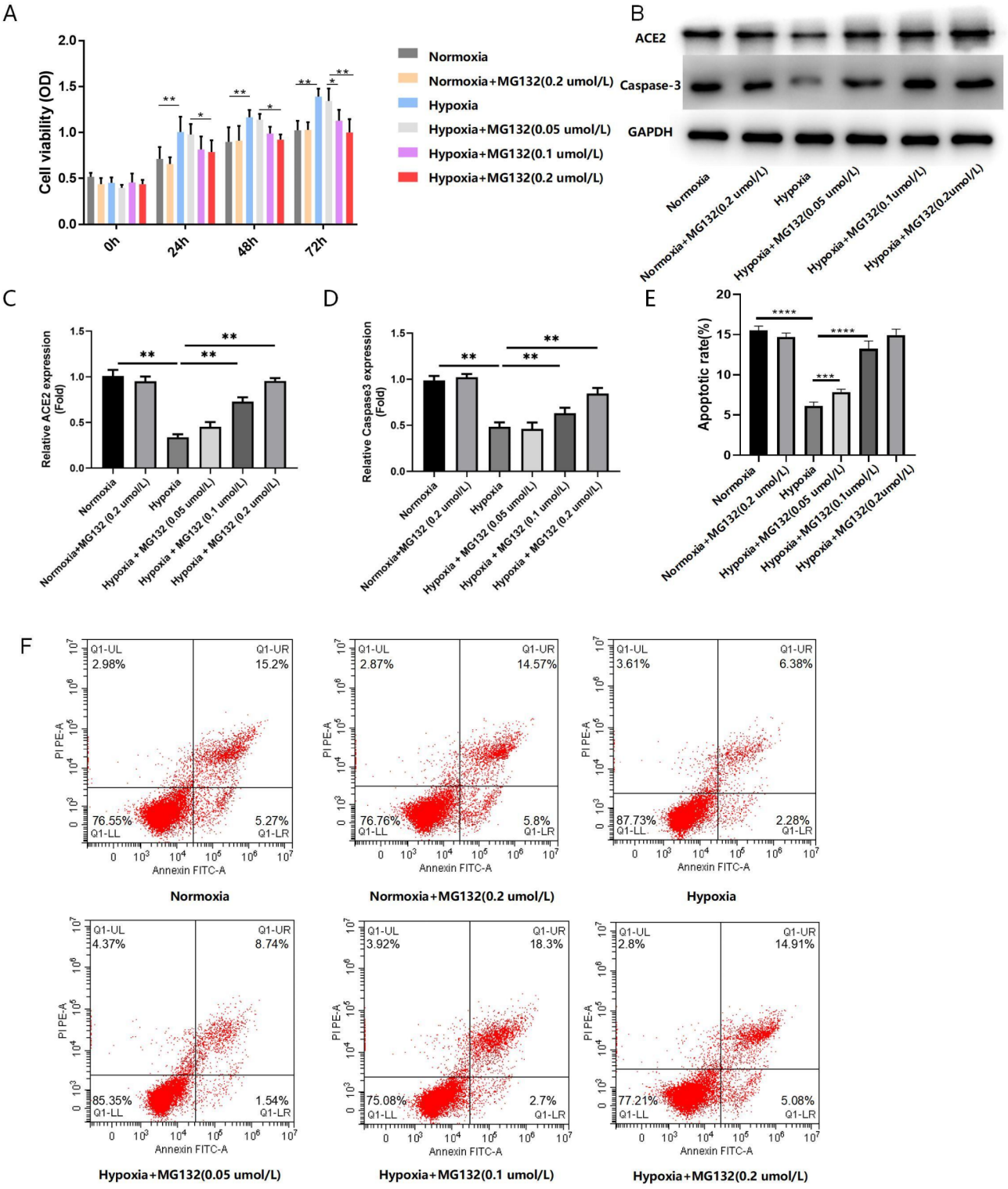

Fig. 3 Ubiquitination promotes the hypoxia-induced proliferation of PASMCs. PASMCs were subjected to hypoxia or normoxia according to the protocol and were treated with low (0.05 μmol/L), medium (0.1 μmol/L), or high (0.2 μmol/L) doses of MG132. MG132, a proteasome inhibitor, can inhibit proteasome-mediated protein degradation via ubiquitination. The effects of ubiquitination on PASMCs viability (**A**) and the expression of ACE2 (**B**, **C**) and caspase-3 (**B**, **D**) were investigated to determine the role of ubiquitination in PVR. GAPDH was used as an internal reference. We then observed apoptosis of each group of PASMCs by flow cytometry, and the proportion of apoptotic cells is shown in (**E**), with representative images (**F**). The percentage of apoptotic cells was defined as the sum of early apoptotic cells and late apoptotic cells. $n = 6$, $^{*}P < 0.05$, $^{**}P < 0.01$. PVR, pulmonary vascular resistance; PASMCs, pulmonary arterial smooth muscle cells; ACE2, angiotensin-converting enzyme 2; GAPDH, glyceraldehyde-3-phosphate dehydrogenase

significantly (Fig. 2E-H). Since there have been no studies on the correlation between NEDD4L and PAH in the literature, we selected NEDD4L for further research.

Hypoxia is accompanied by high expression of NEDD4L and reduced expression of ACE2

HE staining revealed that the number of fully muscular small arteries in the patients with PAH was significantly greater than that in the control group (Fig. 1A-B). Similarly, compared with those in the control group, the proportions of media fraction thickness in the treated group were also significantly greater (Fig. 1A, C). The expression of NEDD4L in the lung tissue of patients with PAH increased ($P<0.01$), the expression of ACE2 decreased ($P<0.01$, Fig. 1D-F), and the expression trend of the two genes correlated negatively ($P=0.028$, $r=-0.4477$, Fig. 1G). We analyzed the expression of NEDD4L and ACE2 in the GEO database for the PH group and the control group by Pearson correlation analysis and found a negative correlation between NEDD4L and ACE2 ($P=0.04$, $r=-0.34$; Fig. 1H).

The expression of NEDD4L negatively correlates with that of ACE2 in PASMCs under hypoxia

After NEDD4L-siRNA transfection, the expression of NEDD4L in PASMCs decreased, indicating that NEDD4L-siRNA was successfully constructed (Fig. 4A, B). After NEDD4L-overexpression(OE) transfection, the protein expression of NEDD4L was significantly increased, indicating that NEDD4L-OE was successfully constructed (Fig. 4C, D). After transfection with NEDD4L-siRNA, ACE2 expression was significantly increased. However, after transfection with NEDD4L-OE, ACE2 expression was significantly decreased (Fig. 4E, G). Then, we observed that cell viability increased to varying degrees in each group over time. At 72 h, the viability of the NEDD4L-OE group was significantly greater than that of the other groups, while the viability of the NEDD4L-siRNA group was significantly lower than that of the other groups (Fig. 4H). Finally, we observed PASMCs apoptosis by flow cytometry and found that the percentage of apoptotic cells in the NEDD4L-siRNA group was significantly greater than that in the control-siRNA group and the control-OE group. The percentage of apoptotic cells in the NEDD4L-OE group was significantly lower than that in the control-siRNA group and the control-OE group, indicating that NEDD4L has a partial inhibitory effect on PASMCs apoptosis (Fig. 4I, J).

Overexpression of ACE2 reverses the inhibition of ACE2 expression by NEDD4L and decreases PASMCs activity and proliferation

To further determine whether NEDD4L promotes PASMC activity and proliferation by inhibiting ACE2 expression, we subjected PASMCs to two treatments, namely NEDD4L overexpression and NEDD4L+ACE2 overexpression. After transfection with NEDD4L-OE, the expression of ACE2 in PASMCs decreased, and the expression of NEDD4L increased. However, after transfection with NEDD4L-OE+ACE2-OE, the expression of ACE2 increased (Fig. 5B, C), and the expression of NEDD4L decreased compared with those in the NEDD4L-OE group (Fig. 5A, C). We used IF staining to examine the expression of ACE2 in PASMCs, and observed this phenomenon (Fig. 5I, K). The CCK-8 results showed that overexpression of NEDD4L promoted the proliferation of PASMCs, while NEDD4L-OE+ACE2-OE reversed this effect (Fig. 5D). EdU staining was used to observe the proliferation of PASMCs. Similar to the CCK-8 results, the proliferation of PASMCs transfected with NEDD4L-OE increased, while the proliferation of PASMCs transfected with NEDD4L-OE+ACE2-OE decreased (Fig. 5J, L). We observed apoptosis of PASMCs by flow cytometry. PASMCs treated with NEDD4L-OE exhibited decreased apoptosis, whereas ACE2-OE partially reversed this effect (Fig. 5E-H).

NEDD4L may inhibit ACE2 expression through ubiquitination

Co-IP experiments were conducted in HEK293 cells (Fig. 6A) and PASMCs (Fig. 6B), and the binding of NEDD4L to ACE2 via ubiquitination was evaluated. In HEK293 cells, compared with those in the control siRNA group, we found significant downregulation of ACE2 ubiquitination and upregulation of ACE2 expression after NEDD4L siRNA intervention. Similarly, NEDD4L and ACE2 coprecipitated in PASMCs. These results indicate that NEDD4L can act as an E3 ubiquitination ligase to regulate the ubiquitination-mediated degradation of ACE2(Fig. 6C).

Discussion

Our experiments demonstrated that (1) inhibition of ubiquitination attenuated hypoxia-induced proliferation of PASMCs; (2) NEDD4L was the E3 ligase of ACE2; (3) in patients with PAH, the expression of NEDD4L increased, while the expression of ACE2 decreased, which were negatively correlated; and (4) NEDD4L inhibited the expression of ACE2 in PASMCs, possibly through ubiquitination-mediated degradation.

Our results showed that hypoxia promoted cell viability and inhibited the expression of ACE2 and caspase-3 in lung tissue, while MG132 reversed these effects in a dose-dependent manner. This finding is consistent with previous studies that have shown that chronic hypoxia can upregulate proteasome activity and promote the proliferation of PASMCs [30–33]. The proteasome inhibitor MG-132 can inhibit the proliferation and migration

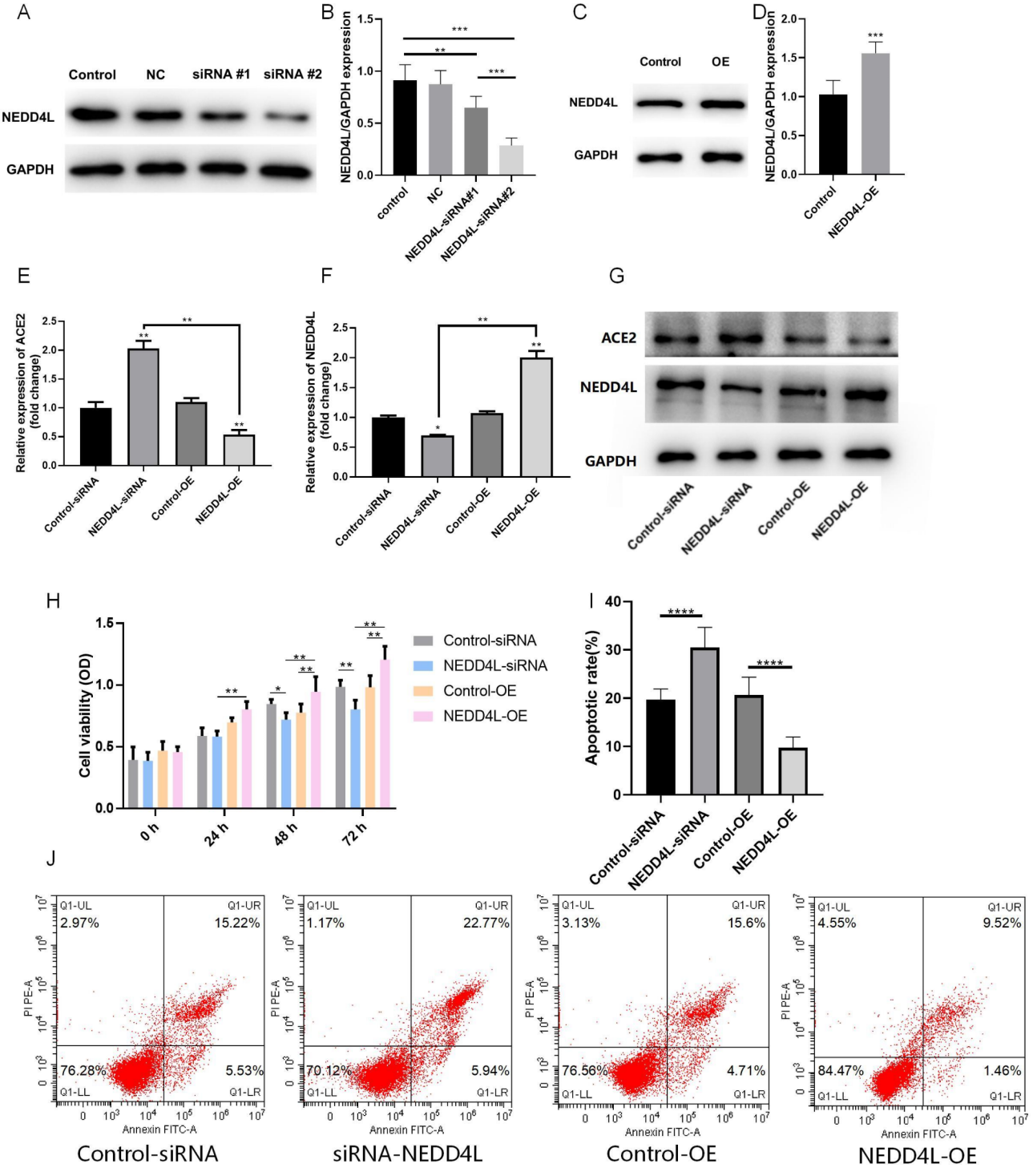

Fig. 4 Effects of NEDD4L inhibition or overexpression on ACE2 protein expression. NEDD4L siRNA (**A-B**) and NEDD4L-OE (**C-D**) were constructed and transfected into PASMCs to examine the expression of NEDD4L. Plasmid transfection was carried out in accordance with the manufacturer's protocol, and the protein expression of ACE2 (**E**, **G**) and NEDD4L (**F**, **G**), cell viability (**H**), and apoptosis (**I-J**) were evaluated. GAPDH was used as an internal reference for western blotting. $N=6$, $^{*}P<0.05$, $^{**}P<0.01$, **** $P<0.0001$. NEDD4L, neural precursor cell–expressed developmentally downregulated gene 4-like; ACE2, angiotensin-converting enzyme 2; PAH, pulmonary arterial hypertension; GAPDH, glyceraldehyde-3-phosphate dehydrogenase

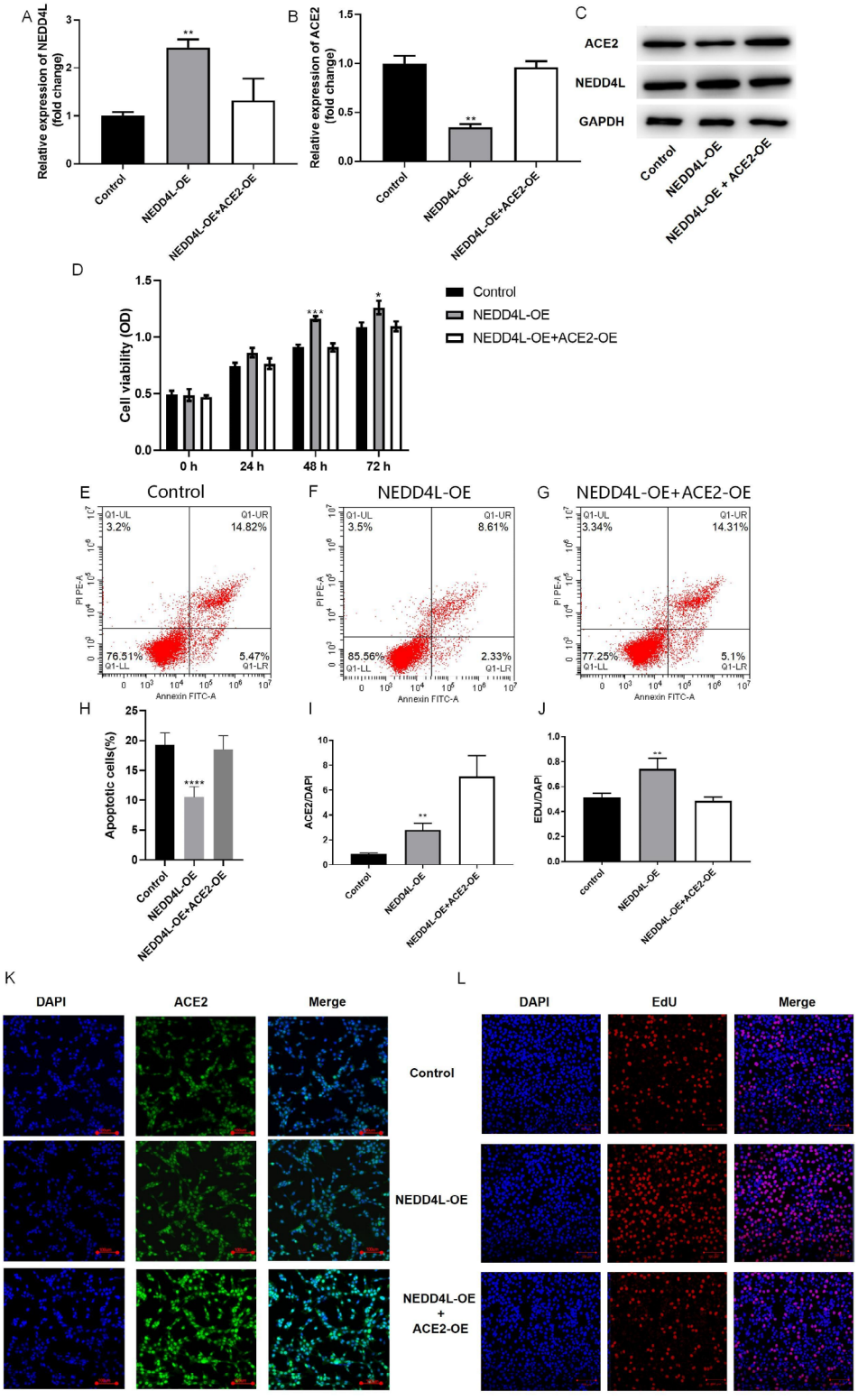

Fig. 5 Overexpression(OE) of ACE2 can partially reverse the inhibition of cell apoptosis by NEDD4L. PASMCs in the two groups were treated with NEDD4L or NEDD4L + ACE2. The expression of NEDD4L and ACE2 in the three groups was examined (**A-C**). Then, PAMSCs were aspirated at 0, 24, 48, and 72 h after transfection, and their cell activity was examined through a CCK-8 assay (**D**). Cell apoptosis was observed by flow cytometry (**E-H**). Finally, IF (**I**, **K**) and EdU (**J**, **L**) staining were performed to observe the expression of ACE2 and cell proliferation in PASMCs. $n = 6$, $^{*}P < 0.05$, $^{**}P < 0.01$, $^{***}P < 0.001$, $^{****}P < 0.0001$. NEDD4L, neural precursor cell–expressed developmentally downregulated gene 4-like; ACE2, angiotensin-converting enzyme 2; PAH, pulmonary arterial hypertension; GAPDH, glyceraldehyde-3-phosphate dehydrogenase

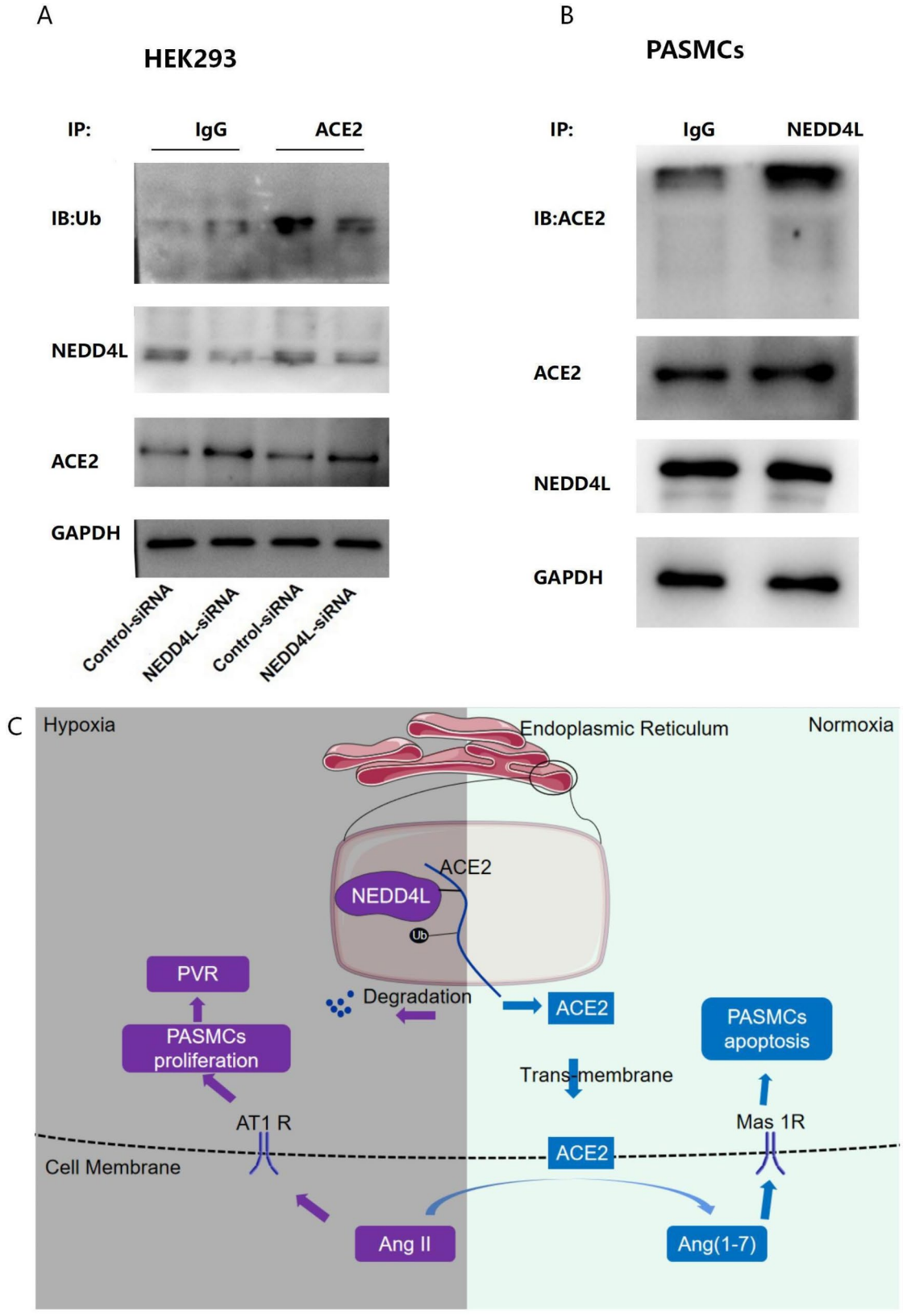

Fig. 6 (See legend on next page.)

(See figure on previous page.)

Fig. 6 NEDD4L may inhibit ACE2 expression through ubiquitination. Before Co-IP, HEK293 cells were transfected with ACE2 and ubiquitin-overexpressing plasmids (1 μg/mL) for 48 h, and then, control-siRNA and NEDD4L-siRNA (20 nM) were added for 24 h. After that, HEK293 cells were treated with MG132 for 10 h (**A**). Before Co-IP, PASMCs were treated with MG132 for 10 h (**B**). A correlation between NEDD4L and ACE2 was detected in HEK293 cells (**A**) and PASMCs (**B**) by co-IP. The mechanism by which NEDD4L-mediated ubiquitination of ACE2 affects PAH (**C**). Inhibiting the expression of NEDD4L can reduce its ability to bind to ACE2 via ubiquitination, thereby increasing the expression of ACE2, promoting the apoptosis of PASMCs, and alleviating pulmonary vascular remodeling. IgG, immunoglobulin G; IP, immunoprecipitation; IB, immunoblotting; Ub, ubiquitin; NEDD4L, neural precursor cell–expressed developmentally downregulated gene 4-like; ACE2, angiotensin-converting enzyme 2; GAPDH, glyceraldehyde-3-phosphate dehydrogenase; PASMCs, pulmonary arterial smooth muscle cells; HEK293, human embryonic kidney 293

of PASMCs, thereby affecting PVR [34]. Pretreatment of PASMCs with MG-132 can inhibit hypoxia-induced cell proliferation to some extent [35]. Our results revealed that MG-132 inhibited hypoxia-induced proliferation of PASMCs.

We then screened the E3 ubiquitination enzymes of ACE2 and selected NEDD4L as a research target. Our previous study showed that hypoxia inhibited the expression of ACE2 in PASMCs, but we did not reveal the underlying mechanism [9]. NEDD4L, the E3 enzyme of ACE2, has been widely studied in various pathophysiological processes of cardiovascular diseases (such as hypertension, myocardial hypertrophy, and heart failure) [25, 36, 37]. However, there have been no studies on NEDD4L in PAH. According to a study on right-heart failure, microRNA-454 can inhibit the expression of NEDD4L, thereby exerting a protective effect on myocardial cells [38]. This suggests that NEDD4L may be highly expressed in PASMCs in PAH, given the correlation between PAH and right-heart failure [39].

In this study, we found that the expression of NEDD4L increased and the expression of ACE2 decreased in the lung tissue of PAH patients, and there was a negative correlation between the two. Zhu reported increased expression of NEDD4L in the lung tissue of rats with PAH induced by monocrotaline, which is consistent with our study [40]. NEDD4L-mediated ubiquitination-based degradation of ACE2 could lead to hypertension [41–43], and this result is also consistent with our study.

The inhibition of ACE2 by NEDD4L was verified by transfecting PASMCs with NEDD4L-siRNA, NEDD4L-OE, or ACE2-OE. NEDD4L-mediated ubiquitination-based degradation of ACE2 has been confirmed in COVID-19 infection [44], and correlation between NEDD4L and ACE2 has further been demonstrated in COVID-19–induced vascular inflammation [45]. Due to the close correlation between PAH and vascular inflammation [23], a decrease in ACE2 is one of the mechanisms underlying the development of PAH [46, 47]. We hypothesized that the ubiquitination-mediated degradation of ACE2 by NEDD4L may inhibit PVR in PAH by reducing vascular inflammation.

This study had many shortcomings. As shown in Fig. 1G/H, there was a negative correlation between ACE2 and NEDD4L expression levels, and we constructed the following regression curves: $Y=-1.448X+3.676$ in Fig. 1G ($R^2=0.2005$) and $Y=-0.41X+5.13$ in Fig. 1H ($R^2=0.115$). No correlation between NEDD4L and ACE2 in PAH has been reported to date. Hypoxia, the mechanism of hypoxic PH, can lead to pulmonary edema [48]. Hypoxia impairs epithelial sodium channel (ENaC) activity and alveolar Na^+ absorption and transport, probably by reducing ENaC expression at the apical membrane of alveolar epithelial cells [49]. NEDD4L mediates the hypoxia-induced decrease in ENaC in alveolar epithelial cells and inhibits amiloride-sensitive Na^+ currents across the apical membrane [50]. Supplementation with hACE2 in vitro can activate ENaC, attenuate reactive oxygen species and tissue-factor generation, and restore barrier function in human lung microvascular endothelial cell (HL-MVEC) monolayers [51]. Amiloride, a prototypical inhibitor of ENaC, can be an ideal candidate for COVID-19 patients because of its ability to increase ACE2 levels and increase the cytosolic pH [52]. Moreover, in our cellular experiments, we found that NEDD4L and ACE2 were strongly negatively correlated. We believe that this unexpected result may be related to the sample processing of lung tissue, where instrumental limitations led to errors in not separating PASMCs from other cells in the lungs. PASMCs were also not separated in the database we selected.

Due to limited research time and tools, we completed only cell experiments and partial clinical studies without performing animal experiments. Further validation of ubiquitination is necessary.

Conclusions

PAH is associated with upregulation of NEDD4L expression and downregulation of ACE2 expression. NEDD4L, the ubiquitination E3 enzyme of ACE2, promotes the proliferation of PASMCs, ultimately leading to PVR. Our present study provides an important experimental basis for NEDD4L as a potential target to treat patients suffered from PAH.

Supplementary Information

The online version contains supplementary material available at https://doi.org/10.1186/s12931-024-02953-5.

Supplementary Material 1: Table S1. Sequences of Primers Used for qPCR

Supplementary Material 2: Fig. 1. Results of the isolation and cultivation of PASMCs. Cell morphology was observed under an inverted phase-contrast microscope, and a cell growth curve was plotted by cell counting

and observed under ×40 and ×100 mirrors (A). Immunofluorescence staining of α-smooth muscle actin (α-SMA) was used to assess the cell type and purity of PASMCs and A549 cells (control, CL0024, Fenghuishengwu, China), which were observed at ×100 and ×200 (B)

Acknowledgements
The authors thank the National Registration Centre for Lung Transplant Data. We are grateful to all the investigators of the study for the data and sample collection.

Author contributions
Conceptualization: Rui Wang 1, Zhiping Wang; Formal analysis: Rui Wang 1, Rui Wang 2; Investigation: Rui Wang 1, Rui Wang 2, Tianya Liu, Jingjing Dang; Provision of study materials or patients: Jingyu Chen; Sample Collection: Tianya Liu, Qianmin Chen; Resources and Funding: Zhiping Wang; Writing (original draft): Rui Wang 1; Review & Editing: Siqi Zhou. All authors participated in writing, reviewing, and editing the manuscript. All authors read and approved the final manuscript.

Funding
This work was supported by the National Natural Science Foundation of China 82270059, Natural Science Foundation of Jiangsu Province BK20221222, and the Jiangsu Provincial Medical Innovation Center CXZX202211.

Data availability
No datasets were generated or analysed during the current study.

Declarations

Ethics approval and consent to participate
This study was performed in accordance with the principles of the Declaration of Helsinki. Approval was granted by the Ethics Committee of the Affiliated Hospital of Xuzhou Medical University (Date 2022-11-21/No. XYFY2022-KL401-01). Informed consent was obtained from all individual participants included in the study.

Consent for publication
Not applicable.

Patient and public involvement
Not applicable.

Competing interests
The authors declare no competing interests.

Received: 22 April 2024 / Accepted: 14 August 2024
Published online: 29 August 2024

References

1. Ruopp NF, Cockrill BA. Diagnosis and treatment of pulmonary arterial hypertension: a review. JAMA. 2022;327(14):1379–91. https://doi.org/10.1001/jama.2022.4402
2. Li H, Li X, Hao Y, et al. Maresin 1 intervention reverses experimental pulmonary arterial hypertension in mice. Eur J Pharmacol. 2022;179(22):5132–47. https://doi.org/10.1111/bph.15906
3. Coons JC, Pogue K, Kolodziej AR, Hirsch GA, George MP. Pulmonary arterial hypertension: a pharmacotherapeutic update. Curr Cardiol Rep. 2019;21(11):141. https://doi.org/10.1007/s11886-019-1235-4
4. Thompson AAR, Lawrie A. Targeting vascular remodeling to treat pulmonary arterial hypertension. Trends Mol Med. 2017;23(1):31–45. https://doi.org/10.1016/j.molmed.2016.11.005
5. Lu X, Zhang J, Liu H, et al. Cannabidiol attenuates pulmonary arterial hypertension by improving vascular smooth muscle cells mitochondrial function. Theranostics. 2021;11(11):5267–78. https://doi.org/10.7150/thno.55571
6. Li M, Ying M, Gu S, Zhou Z, Zhao R. SIRT6 inhibits hypoxia-induced pulmonary arterial smooth muscle cells proliferation via HIF-1α/PDK4 signaling. Life Sci. 2023;312:121192. https://doi.org/10.1016/j.lfs.2022.121192
7. Hu P, Xu Y, Jiang Y, et al. The mechanism of the imbalance between proliferation and ferroptosis in pulmonary artery smooth muscle cells based on the activation of SLC7A11. Eur J Pharmacol. 2022;928:175093. https://doi.org/10.1016/j.ejphar.2022.175093
8. Hassoun PM. Pulmonary arterial hypertension. N Engl J Med. 2021;385(25):2361–76. https://doi.org/10.1056/NEJMra2000348
9. Wang R, Xu J, Wu J, Gao S, Wang Z. Angiotensin-converting enzyme 2 alleviates pulmonary artery hypertension through inhibition of focal adhesion kinase expression. Experimental Therapeutic Med. 2021;22(4):1165. https://doi.org/10.3892/etm.2021.10599
10. Donoghue M, Hsieh F, Baronas E, et al. A novel angiotensin-converting enzyme-related carboxypeptidase (ACE2) converts angiotensin I to angiotensin 1–9. Circul Res. 2000;87(5):E1–9. https://doi.org/10.1161/01.res.87.5.e1
11. De Man FS, Tu L, Handoko ML, et al. Dysregulated renin-angiotensin-aldosterone system contributes to pulmonary arterial hypertension. Am J Respir Crit Care Med. 2012;186(8):780–9. https://doi.org/10.1164/rccm.201203-0411OC
12. Dai H, Jiang L, Xiao Z, Guang X. ACE2-angiotensin-(1–7)-Mas axis might be a promising therapeutic target for pulmonary arterial hypertension. Nat Reviews Cardiol. 2015;12(6):374. https://doi.org/10.1038/nrcardio.2015.6-c1
13. Dai H, Gong Y, Xiao Z, Guang X, Yin X. Decreased levels of serum Angiotensin-(1–7) in patients with pulmonary arterial hypertension due to congenital heart disease. Int J Cardiol. 2014;176(3):1399–401. https://doi.org/10.1016/j.ijcard.2014.08.021
14. Hemnes AR, Rathinasabapathy A, Austin EA, et al. A potential therapeutic role for angiotensin-converting enzyme 2 in human pulmonary arterial hypertension. Eur Respir J. 2018;51(6):1702638. https://doi.org/10.1183/13993003.02638-2017
15. Oliveira AC, Yang T, Li J, et al. Fecal matter transplant from Ace2 overexpressing mice counteracts chronic hypoxia-induced pulmonary hypertension. Pulmonary Circulation. 2022;12(1):e12015. https://doi.org/10.1002/pul2.12015
16. Cockram PE, Kist M, Prakash S, Chen SH, Wertz IE, Vucic D. Ubiquitination in the regulation of inflammatory cell death and cancer. Cell Death Differ. 2021;28(2):591–605. https://doi.org/10.1038/s41418-020-00708-5
17. Han S, Wang R, Zhang Y, et al. The role of ubiquitination and deubiquitination in tumor invasion and metastasis. Int J Biol Sci. 2022;18(6):2292–303. https://doi.org/10.7150/ijbs.69411
18. Tang H, Gupta A. Deficiency of the deubiquitinase UCHL1 attenuates pulmonary arterial hypertension. Circulation. 2024;150(4):302–16. https://doi.org/10.1161/circulationaha.123.065304
19. Jin S, He X, Ma L, et al. Suppression of ACE2 SUMOylation protects against SARS-CoV-2 infection through TOLLIP-mediated selective autophagy. Nat Commun. 2022;13(1):5204. https://doi.org/10.1038/s41467-022-32957-y
20. Manne BK, Denorme F, Middleton EA, et al. Platelet gene expression and function in patients with COVID-19. Blood. 2020;136(11):1317–29. https://doi.org/10.1182/blood.2020007214
21. Mohammed M, Ogunlade B. Nedd4-2 upregulation is associated with ACE2 ubiquitination in hypertension. Cardiovascular Res. 2023;5(10):cvad070. https://doi.org/10.1093/cvr/cvad070
22. Lazartigues E, Llorens-Cortes C, Danser AHJ. New approaches targeting the renin-angiotensin system: inhibition of brain aminopeptidase A, ACE2 ubiquitination, and angiotensinogen. Can J Cardiol. 2023;282X(23):522–6. https://doi.org/10.1016/j.cjca.2023.06.013. S0828-.
23. Hu Y, Chi L, Kuebler WM. Perivascular inflammation in pulmonary arterial hypertension. Cells. 2020;9(11):2338. https://doi.org/10.3390/cells9112338
24. Wang RR, Yuan TY, Wang JM, et al. Immunity and inflammation in pulmonary arterial hypertension: from pathophysiology mechanisms to treatment perspective. Pharmacol Res. 2022;180(1):106238. https://doi.org/10.1016/j.phrs.2022.106238
25. Li M, Sun G, Wang P, et al. Research progress of Nedd4L in cardiovascular diseases. Cell Death Discovery. 2022;8(1):206. https://doi.org/10.1038/s41420-022-01017-1
26. Cuijpers SAG, Willemstein E, Vertegaal ACO. Converging small ubiquitin-like modifier (SUMO) and Ubiquitin Signaling: Improved Methodology identifies co-modified Target proteins. Mol Cell Proteom. 2017;16(12):2281–95. https://doi.org/10.1074/mcp.TIR117.000152
27. Zhu Y, Wu Y, Shi W, et al. Inhibition of ubiquitin proteasome function prevents monocrotaline-induced pulmonary arterial remodeling. Life Sci. 2017;173(1):36–42. https://doi.org/10.1016/j.lfs.2017.02.007
28. Shen H, Zhang L, Yao D, Zhang Z, Gong K. [Hypoxia enhances proliferation and migration of mouse pulmonary artery smooth muscle cells in vitro]. Xi bao Yu Fen Zi Mian Yi Xue Za Zhi = Chinese. J Cell Mol Immunol. 2019;35(1):39–45.

29. Xu J, Li X, Zhou S, et al. Inhibition of CXCR4 ameliorates hypoxia-induced pulmonary arterial hypertension in rats. Am J Translational Res. 2021;13(3):1458–70.
30. Wang J, Xu L, Yun X, et al. Proteomic analysis reveals that proteasome subunit beta 6 is involved in hypoxia-induced pulmonary vascular remodeling in rats. PLoS ONE. 2013;8(7):e67942. https://doi.org/10.1371/journal.pone.0067942
31. Sulkshane P, Ram J, Thakur A, Reis N, Kleifeld O, Glickman MH. Ubiquitination and receptor-mediated mitophagy converge to eliminate oxidation-damaged mitochondria during hypoxia. Redox Biol. 2021;45(1):102047. https://doi.org/10.1016/j.redox.2021.102047
32. Feng R, Mayuranathan T, Huang P. Activation of γ-globin expression by hypoxia-inducible factor 1α. Nature. 2022;610(7933):783–90. https://doi.org/10.1038/s41586-022-05312-w
33. Liu R, Xu C, Zhang W, et al. FUNDC1-mediated mitophagy and HIF1α activation drives pulmonary hypertension during hypoxia. Cell Death Dis. 2022;13(7):634. https://doi.org/10.1038/s41419-022-05091-2
34. Liu H, Ge XY, Huang N, et al. Up-regulation of cullin7 promotes proliferation and migration of pulmonary artery smooth muscle cells in hypoxia-induced pulmonary hypertension. Eur J Pharmacol. 2019;864:172698. https://doi.org/10.1016/j.ejphar.2019.172698
35. Zhu Y, Zhang Q, Yan X, et al. Ubiquitin-specific protease 7 mediates platelet-derived growth factor-induced pulmonary arterial smooth muscle cells proliferation. Pulmonary Circulation. 2021;11(4):20458940211046131. https://doi.org/10.1177/20458940211046131
36. Li H, Wang N, Jiang Y. E3 ubiquitin ligase NEDD4L negatively regulates inflammation by promoting ubiquitination of MEKK2. EMBO Rep. 2022;23(11):e54603. https://doi.org/10.15252/embr.202254603
37. Niu ZJ, Yao S, Zhang X, et al. Associations of genetic variations in NEDD4L with salt sensitivity, blood pressure changes and hypertension incidence in Chinese adults. J Clin Hypertens (Greenwich). 2022;24(10):1381–9. https://doi.org/10.1111/jch.14566
38. Wang Y, Pan W, Bai X, Wang X, Wang Y. microRNA-454-mediated NEDD4-2/TrkA/cAMP axis in heart failure: mechanisms and cardioprotective implications. J Cell Mol Med. 2021;25(11):5082–98. https://doi.org/10.1111/jcmm.16491
39. Al-Qazazi R, Lima PDA. Macrophage-NLRP3 activation promotes right ventricle failure in pulmonary arterial hypertension. Am J Respir Crit Care Med. 2022;206(5):608–24. https://doi.org/10.1164/rccm.202110-2274OC
40. Zhu Y, Wu Y, Shi W, et al. Inhibition of ubiquitin proteasome function prevents monocrotaline-induced pulmonary arterial remodeling. Life Sci. 2017;173:36–42. https://doi.org/10.1016/j.lfs.2017.02.007
41. Mohammed M, Ogunlade B. Nedd4-2 upregulation is associated with ACE2 ubiquitination in hypertension. Cardiovascular Research. 2023; 2023(5):1–12. https://doi.org/10.1093/cvr/cvad070
42. Kong D, Wan Q, Li J, et al. DP1 activation reverses Age-Related Hypertension Via NEDD4L-Mediated T-Bet degradation in T cells. Circulation. 2020;141(8):655–66. https://doi.org/10.1161/circulationaha.119.042532
43. Ishigami T, Kino T, Minegishi S, Araki N, Umemura M. Regulators of epithelial Sodium channels in Aldosterone-Sensitive Distal nephrons (ASDN): critical roles of Nedd4L/Nedd4-2 and salt-sensitive hypertension. Int J Mol Sci. 2020;21(11):3871. https://doi.org/10.3390/ijms21113871
44. Wen K, Bai C, Zhao H, et al. Low dose radiation therapy attenuates ACE2 depression and inflammatory cytokines induction by COVID-19 viral spike protein in human bronchial epithelial cells. Int J Radiat Biol. 2022;98(10):1532–41. https://doi.org/10.1080/09553002.2022.2055806
45. Birch CA, Molinar-Inglis O, Trejo J. Subcellular hot spots of GPCR signaling promote vascular inflammation. Curr Opin Endocr Metabolic Res. 2021;16(1):37–42. https://doi.org/10.1016/j.coemr.2020.07.011
46. Chatterjee P, Gheblawi M, Wang K, Vu J, Kondaiah P, Oudit GY. Interaction between the apelinergic system and ACE2 in the cardiovascular system: therapeutic implications. Clin Sci. 2020;134(17):2319–36. https://doi.org/10.1042/cs20200479
47. Sandoval J, Del Valle-Mondragón L. Angiotensin converting enzyme 2 and angiotensin (1–7) axis in pulmonary arterial hypertension. Eur Respir J. 2020;56(1):1902416. https://doi.org/10.1183/13993003.02416-2019
48. Sylvester JT, Shimoda LA, Aaronson PI, Ward JP. Hypoxic pulmonary vasoconstriction. Physiol Rev. 2012;92(1):367–520. https://doi.org/10.1152/physrev.00041.2010
49. Dunham-Snary KJ, Wu D, Sykes EA, et al. Hypoxic pulmonary vasoconstriction: from Molecular mechanisms to Medicine. Chest. 2017;151(1):181–92. https://doi.org/10.1016/j.chest.2016.09.001
50. Gille T, Randrianarison-Pellan N, Goolaerts A, et al. Hypoxia-induced inhibition of epithelial na(+) channels in the lung. Role of Nedd4-2 and the ubiquitin-proteasome pathway. Am J Respir Cell Mol Biol. 2014;50(3):526–37. https://doi.org/10.1165/rcmb.2012-0518OC
51. Romero MJ, Yue Q, Singla B, et al. Direct endothelial ENaC activation mitigates vasculopathy induced by SARS-CoV2 spike protein. Front Immunol. 2023;14:1241448. https://doi.org/10.3389/fimmu.2023.1241448
52. Adil MS, Narayanan SP, Somanath PR. Is amiloride a promising cardiovascular medication to persist in the COVID-19 crisis? Drug discoveries and therapeutics. 2020; 14(5):256–8. https://doi.org/10.5582/ddt.2020.03070

Publisher's note